Supporting Information

The twinned Pd nanocatalyst exhibits sustainable NRR electrocatalytic performance by promoting the desorption of NH_3

Wenwen Cai,[a] Yi Han,[a] Yue Pan,[a] Xinyi Zhang,[a] Jixiang Xu,[a] Yanyun Zhang,[a] Yuyao Sun,[a] Shaoxiang Li,[b]

Jianping Lai*,[a] and Lei Wang*,[a,b]

[a]Key Laboratory of Eco-chemical Engineering, Ministry of Education, Taishan scholar advantage and characteristic discipline team of Ecochemical progress and technology, Laboratory of Inorganic Synthesis and Applied Chemistry, College of Chemistry and Molecular Engineering, Qingdao University of Science and Technology, Qingdao 266042, P. R. China.

[b]Shandong Engineering Research Center for Marine Environment Corrosion and Safety Protection, College of Environment and Safety Engineering, Qingdao University of Science and Technology, Qingdao 266042, P. R. China.

Correspondence and requests for materials should be addressed to J.L. (e-mail: jplai@qust.edu.cn) and L.W. (e-mail: inorchemwl@126.com).

Experimental Section

Materials. $Li_2SO_4 \cdot H_2O$ (99.99%), triethylene glycol (Tri-EG, 98.0%), Diethylene glycol (DEG, 99.0%) and KOH (98%) were purchased from Aladdin (Shanghai, China). HCl (37%) was supplied by Far East Fine Chemicals (Yantai, China). Sodium tetrachloropalladate (II) (Na_2PdCl_4, 98%) was purchased from Sigma-Aldrich. Potassium bromide (KBr, 99%) was purchased from Sinopharm Chemical Reagent Co., Ltd. L-ascorbic acid (AA, 99%) was supplied by Alfer Aesar. All chemicals are of analytical grade and can be used without further purification. Deionized H_2O was used in the whole experiment.

Preparation of Pd Octahedra. The Pd octahedron was synthesized according to the previously reported

two-step method with slight modifications. The first step is to prepare Pd nanocubes with a particle size of about 18 nm. In order to prepare Pd nanocubes, 105 mg PVP, 600 mg KBr, 60 mg AA and 8 mL deionized water were mixed in a pressure bottle under magnetic stirring. After complete dissolution, the bottle was placed in a preheated oil bath at 80 ℃ for magnetic stirring and kept for 10 minutes. Subsequently, 3.0 mL of an aqueous solution containing 57 mg of Na_2PdCl_4 was added to the bottle, and the solution was kept at 80 ℃ for 3 hours and then cooled to room temperature. The product was collected by centrifugation and washed 3 times with deionized water. The second step is to convert Pd nanocubes into Pd octahedrons. First, the Pd nanocubes prepared by the above method were redispersed in 11 mL of Tri-EG. Then, under magnetic stirring, 33.3 mg of PVP, 0.5 mL of Tri-EG solution containing Pd nanocubes and 7.5 mL of Tri-EG were mixed uniformly in a glass vial. Then put the vial into a preheated 130 ℃ oil bath and stir it magnetically for 10 minutes. Subsequently, 70 μL of HCl (37%) was injected into the bottle, and the reaction was continued at 130 ℃ for 2 hours. After completion, the reaction solution was cooled to room temperature. The final product was collected by centrifugation and washed 3 times with deionized water.

Preparation of Pd Icosahedra. Mix 80 mg PVP and 2 mL DEG ultrasonically in a pressure bottle. After being completely dissolved, the glass bottle was placed in a preheated oil bath (115 ℃) and kept stirring for 10 minutes. After that, 1.0 mL of DEG solution containing 15.5 mg of Na_2PdCl_4 was added to the bottle. The reaction was maintained at 115 ℃ under magnetic stirring for 10 hours. Finally, after cooling the reaction solution to room temperature, the final product was collected by centrifugation, and washed with deionized water 3 times.

Characterization. X-ray diffraction (XRD) analysis at a scanning rate of 1° min^{-1} in the 2θ ranges from 5 to 90° was used to evaluate the composition of the as-synthesized samples on X'Pert PRO MPD. Transmission electron microscopy (TEM) and high-resolution TEM (HRTEM) measurements were conducted on JEM-2100UHR with operating at 200 kV. The X-ray photoelectron spectrum (XPS) was performed using a VG ESCALABMK II spectrometer with AlKa (1486.6 eV) photon source. All the electrochemical performances of the as-prepared samples were carried out on an electrochemical station (CHI 760E). The ^1H NMR spectrum was recorded on a Bruker 500 with Probe TXI at temperature of 25 ℃ using a 3 mm tube. The electrolyte after electrolysis was collected, lyophilized and further dissolved in 1 M HCl solution (D_2O/H_2O mixed solution). The IC data were collected by an IC (863 Basic IC Plus. Metrohm, Switzerland) equipped with a Metrosep C Supp 4-250/4.0 column. In suit Fourier transform infrared (FTIR) spectrometer (Nicolet IS50, Thermofisher Scientific) and ATR were used for infrared

spectroscopy.

Electrochemical measurements. All electrochemical measurements were carried out using an electrochemical workstation (Shanghai Chenhua Instrument Corporation, China) and a two-compartment electrochemical cell, which was connected by a salt bridge. The Pd octahedron and Pd icosahedron were deposited on carbon paper as working electrode, carbon rod as counter electrode, saturated calomel electrode (SCE) and saturated KCl electrolyte as reference electrode. All the gas used in this work is with a purity grade of 99.999 % and fully purified by the Cu impurity trap, then aerated into the electrolyte more than 30 min. The potential reported in this work was converted to the RHE scale using the following equation: E(RHE)=E(SCE)+(0.244+0.059×pH)V. For the NRR test, the chronoamperometry experiments were conducted in N_2-saturated 0.1 M Li_2SO_4 solution (Notably, the Li_2SO_4 used was preconditioned at 800 ℃ about 4 h in Ar.) with stirring at 450 rpm. For the preparation of the working electrode, 2 mg catalyst was first dispersed in the mixed solution of 1.0 mL of absolute ethanol and 50 μL of Nafion solution (5.0 wt%) under ultrasonication for 5 min to form a homogeneous catalyst ink. After that, 50 μL of the prepared catalyst ink was loaded onto a commercial carbon paper with an area of 1.0×1.0 cm^2, then dried under ambient conditions for further usage.

Ammonia quantification. The produced NH_3 was quantitatively determined using the indophenol blue method.[1] Typically, 1 mL of the sample solution was first pipetted from the post-electrolysis electrolyte. Afterward, 1 mL of a 1M NaOH solution containing salicylic acid (5 wt%) and sodium citrate (5 wt%) was added, and 0.5 mL of NaClO solution (0.05 M) and 0.1 mL of sodium nitroferricyanide solution (1 wt%) were added subsequently. After 2 h, the absorption spectra of the resulting solution were acquired with an ultraviolet-visible (UV-vis) spectrophotometer (BioTek Synergy H1 Hybrid Multi-Mode Reader). The formed indophenol blue was measured by absorbance at λ = 654 nm. The concentration (NH_4^+) absorbance curve used for estimation of NH_3 amount was calibrated using standard NH_4Cl solution with NH_4^+ concentrations of 0.0, 0.2, 0.4, 0.6, 0.8, and 1.0 μg mL^{-1} in 0.1 M Li_2SO_4. The fitting curve ($y=0.509x+0.04065$, $R^2=0.999$) showed a good linear relation between the NH_4^+ concentration and absorbance.

$^{15}N_2$ isotope labelling experiments. The produced NH_3 was detected by the ^1H NMR. $^{15}N_2$ (99%, provided by the Shanghai Aladdin Biochemical Technology Co., Ltd) was used to further verify the N-source of NH_3 produced. All the gases were purified by the Cu impurity trap. Before the electrolysis, the Ar was plunged into the electrolyte about 1 h, then $^{15}N_2$ was plunged into the electrolyte to saturation. The

electrolyte after electrolysis at -0.2 (V vs. RHE) was collected, lyophilized and further dissolved in the solution of 1 M HCl, D_2O and H_2O. Then the $^{15}NH_3$ produced was detected by the ^1H NMR spectrum (Bruker 500). The procedure that detected $^{14}NH_3$ produced was the same except the $^{14}N_2$ (99.999%) was used. The standard curves was calibrated by using a series of concentrations of NH_4Cl. And the fitting curves are y=0.034x+0.004, R^2=0.999 and y=0.036x-0.002, R^2=0.998.

Determination of hydrazine. The hydrazine present in the electrolyte was estimated by the method of Watt and Chrisp.[2] A mixture of para-(dimethylamino) benzaldehyde (5.99 g), HCI (concentrated, 30 mL) and ethanol (300 mL) was used as a color reagent. The calibration curve was plotted as follow: First, preparing a series of reference solutions, by pipetting suitable volumes of the hydrazine hydrate-nitrogen 0.1 M HCl solution in colorimetric tubes; Second, making up to 5 mL with 0.1 M HCl solution; Third, adding 5 mL above prepared color reagent and stirring 10 min at room temperature; Fourth, the absorbance of the resulting solution was measured at 455 nm, and the obtained calibration curve (y=1.184x+0.02371, R^2=0.999) was used to calculate the hydrazine concentration.

Calculation of the Faradaic efficiency and the yield rate. The faradaic efficiency for N_2 reduction was defined as the amount of electric charge used for synthesizing NH_3 divided the total charge passed through the electrodes during the electrolysis. The total amount of NH_3 produced was measured using colorimetric methods. Assuming three electrons were needed to produce one NH_3 molecule, the FE could be calculated as follows:

Faradaic efficiency (FE,%)=$(3F\times C_{NH4^+}\times V)/(17Q)\times 100\%$

The NH_3 yield was calculated using the following equation:

NH_3 yield=$(C_{NH4+}\times V)/(t\times A)$

where F is the faraday constant, C_{NH4+} is the measured concentration of NH_4^+, V is the electrolyte volume, Q is the sum of electric charge recorded by electrochemical workstation, 17 is the molarmass of NH_4^+ atom, t is the reaction time, and A is the geometric area of the cathode (1 cm^{-2}).

Calculation Setup. To forecast the chemical properties of prepared Pd nanoparticles, the slabs of Pd icosahedron and Pd octahedron were established by 147 and 85 atoms, respectively. DFT calculations of the Pd icosahedron and octahedron slabs were computed by using Vienna ab initio simulation package (VASP) within a generalized gradient approximation (GGA) of exchange-correlation functional in the Perdew, Burke, and Ernzerhof (PBE). A plane-wave energy cut off of 400 eV was used together with norm-conserving pseudopotentials, and the convergence criteria of energy was 10^{-5} eV. The residual force was within 0.01 eV/Å for geometry optimizations. The free energy (G) was computed from:

$$G = E + ZPE - T\Delta S$$

where E was the total energy, ZPE was the zero-point energy, the entropy (ΔS) of each adsorbed state were yielded from DFT calculation, whereas the thermodynamic corrections for gas molecules were from standard tables.

Figures

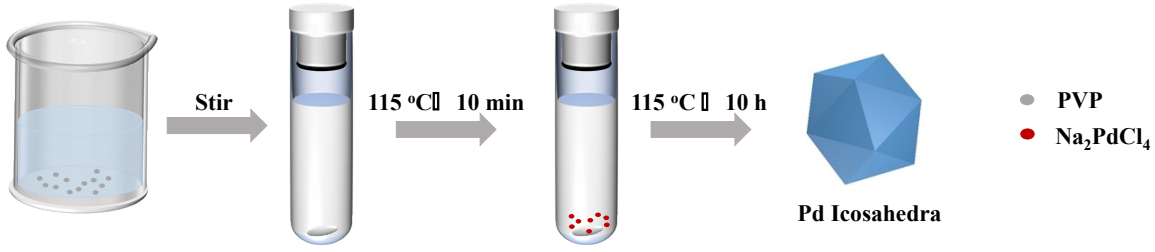

Scheme S1. Synthetic schematic diagram of Pd icosahedron.

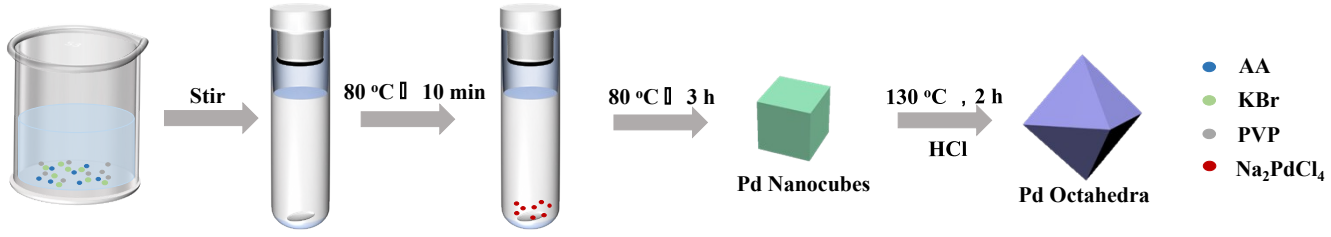

Scheme S2. Synthetic schematic diagram of Pd octahedron.

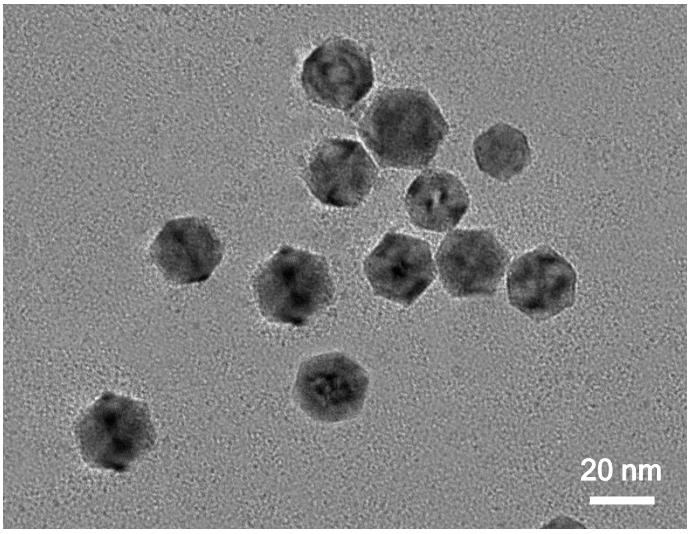

Figure S1. TEM image of Pd icosahedron.

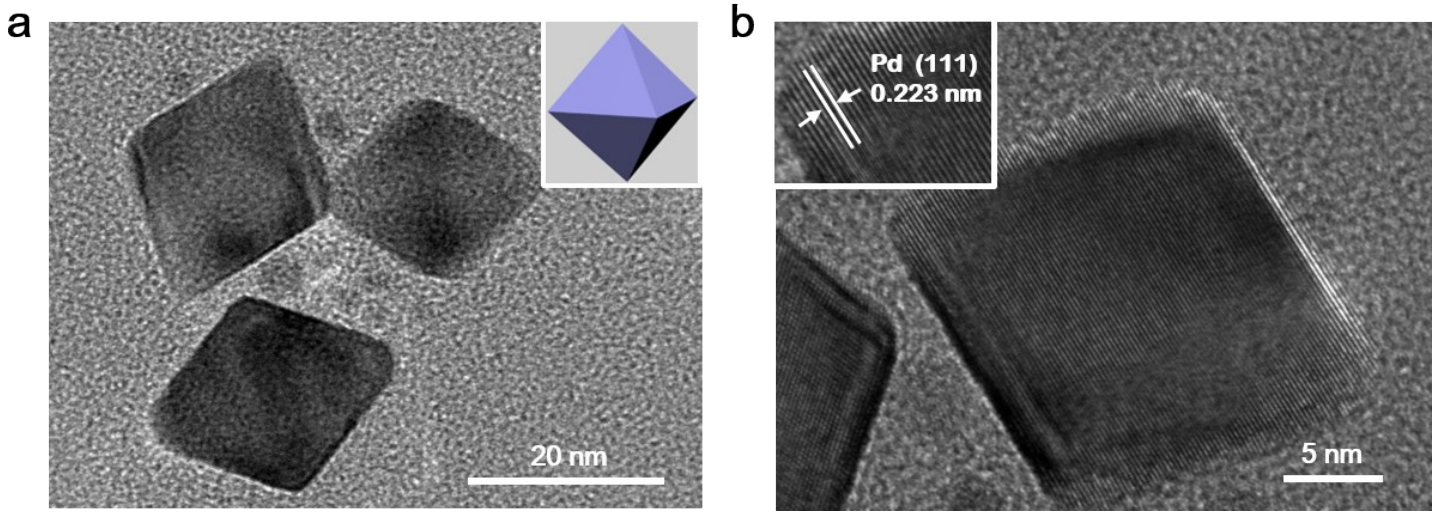

Figure S2. (a) TEM and (b) HRTEM images of Pd octahedrons.

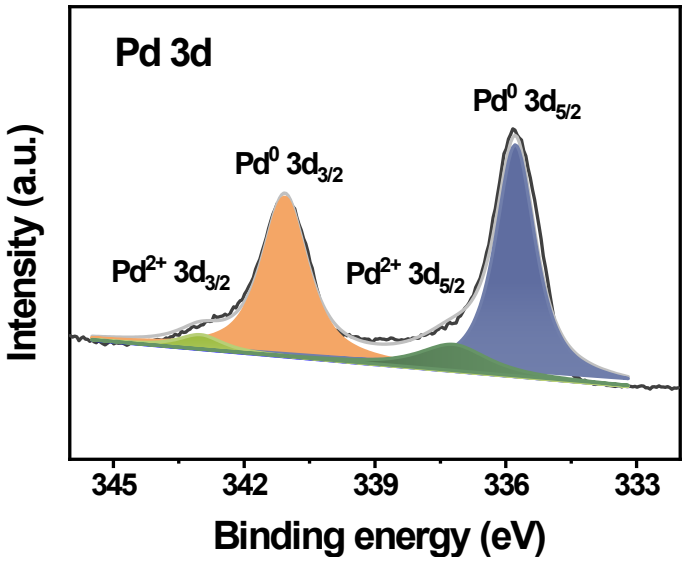

Figure S3. Pd 3d XPS spectra of Pd octahedrons.

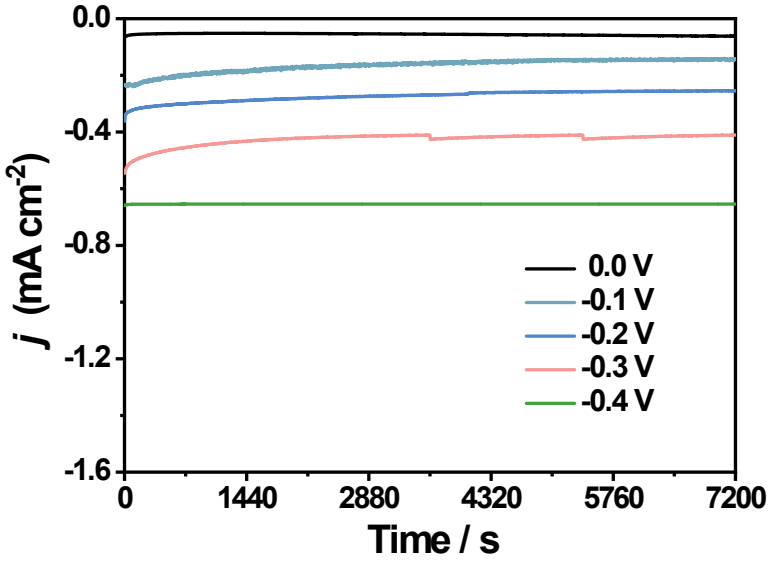

Figure S4. Chronoamperometry curves of Pd icosahedron for 2 h.

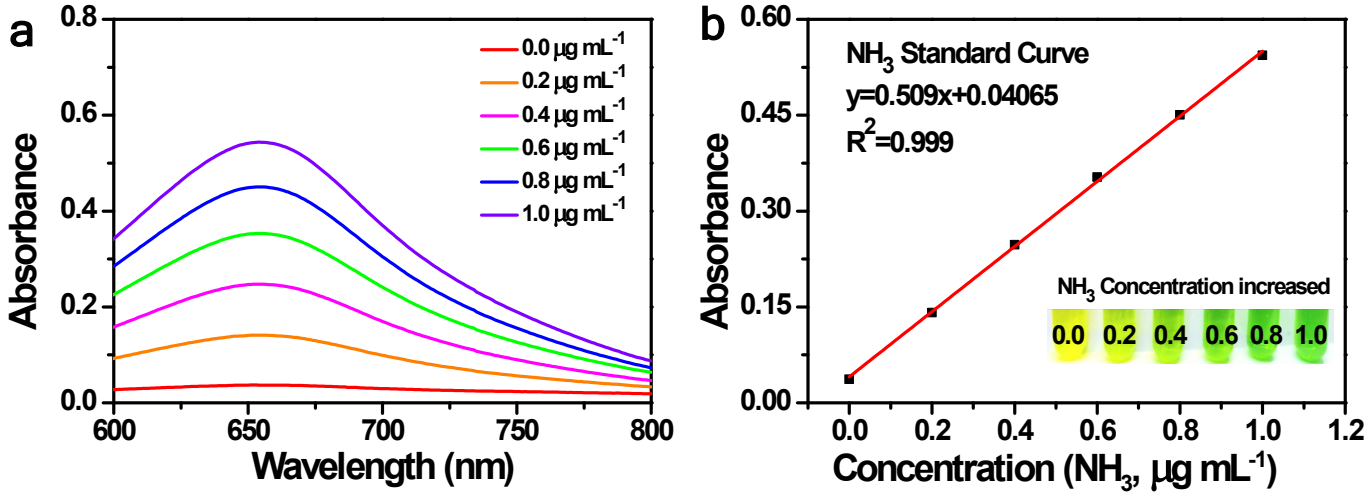

Figure S5. The UV-Vis absorption spectra of indophenol assays with NH_3 after incubated for 2 h at room temperature. (b) Corresponding calibration curves for the colorimetric NH_3 assay in 0.1 M Li_2SO_4.

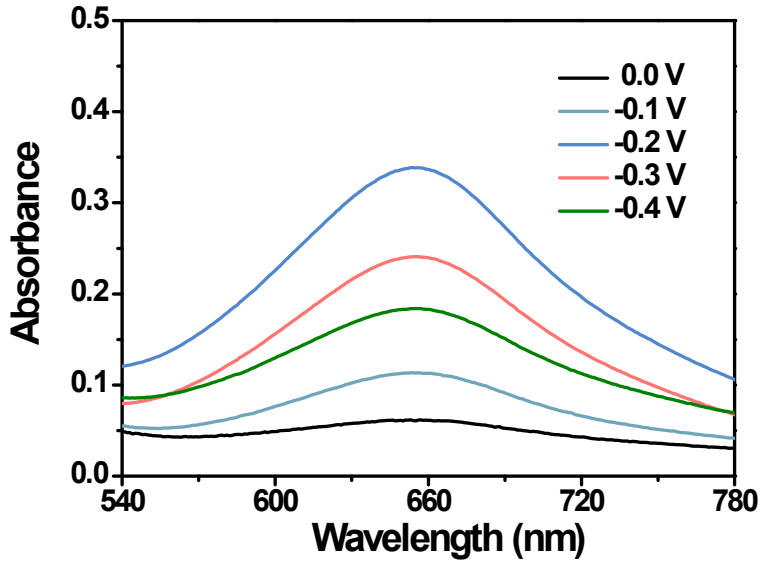

Figure S6. UV-Vis absorption spectra of the 0.1 M Li_2SO_4 electrolyte stained with the indophenol indicator.

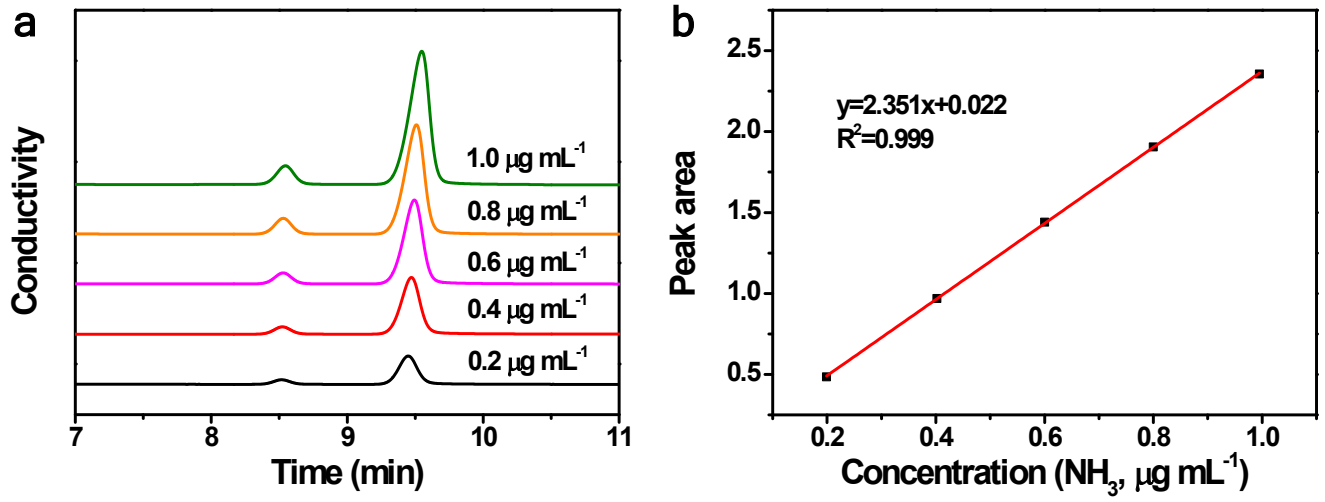

Figure S7. (a) Ion chromatogram analysis for the NH_4^+. (b) Calibration curve used for estimation of NH_4^+.

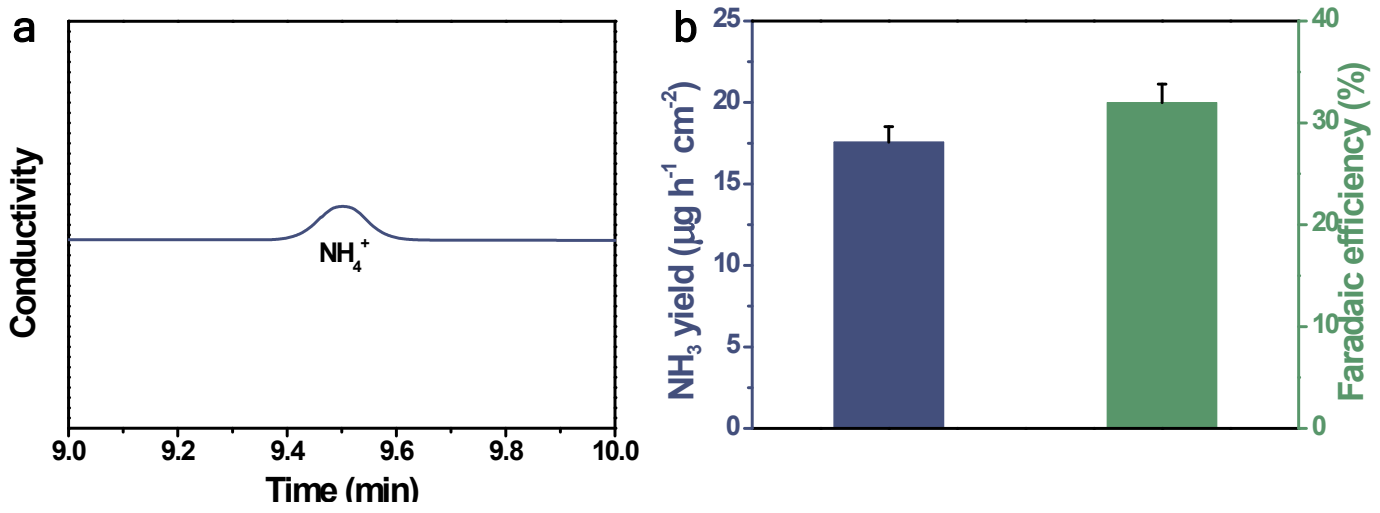

Figure S8. (a) Ion chromatogram analysis for the NH_4^+ of Pd icosahedron. (b) The NH_4^+ yield and FE detected by ion chromatography.

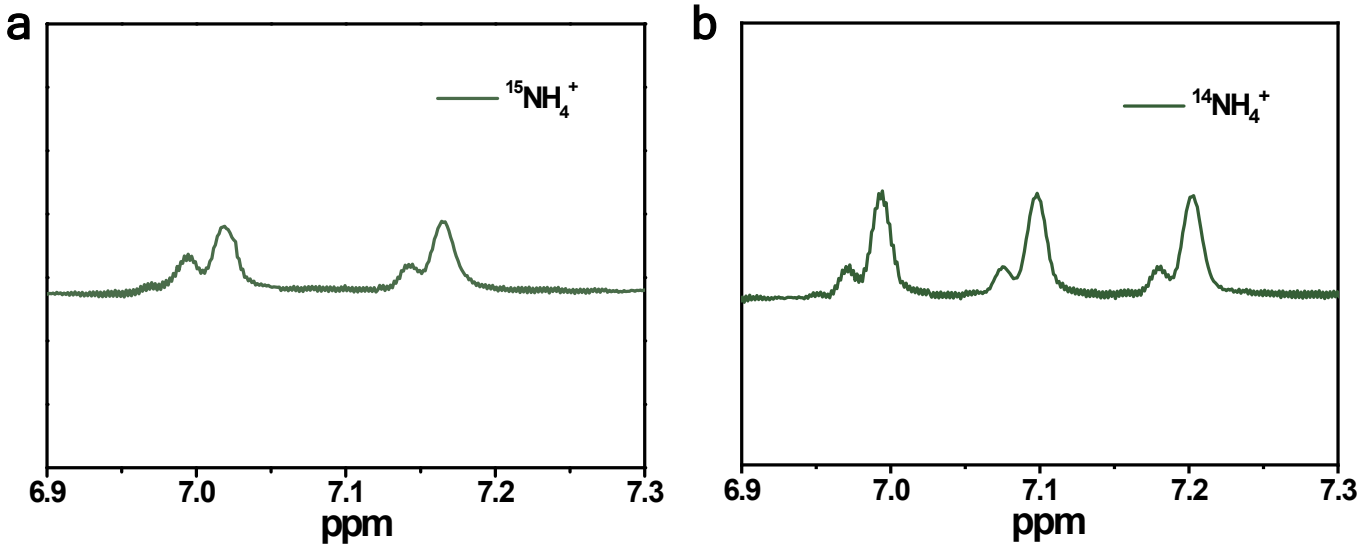

Figure S9. (a) The ^{1}H-NMR spectrum of electrolyte that electrolysis in $^{15}N_2$-saturated condition. (b) The ^{1}H-NMR spectrum of electrolyte that electrolysis $^{14}N_2$-saturated condition.

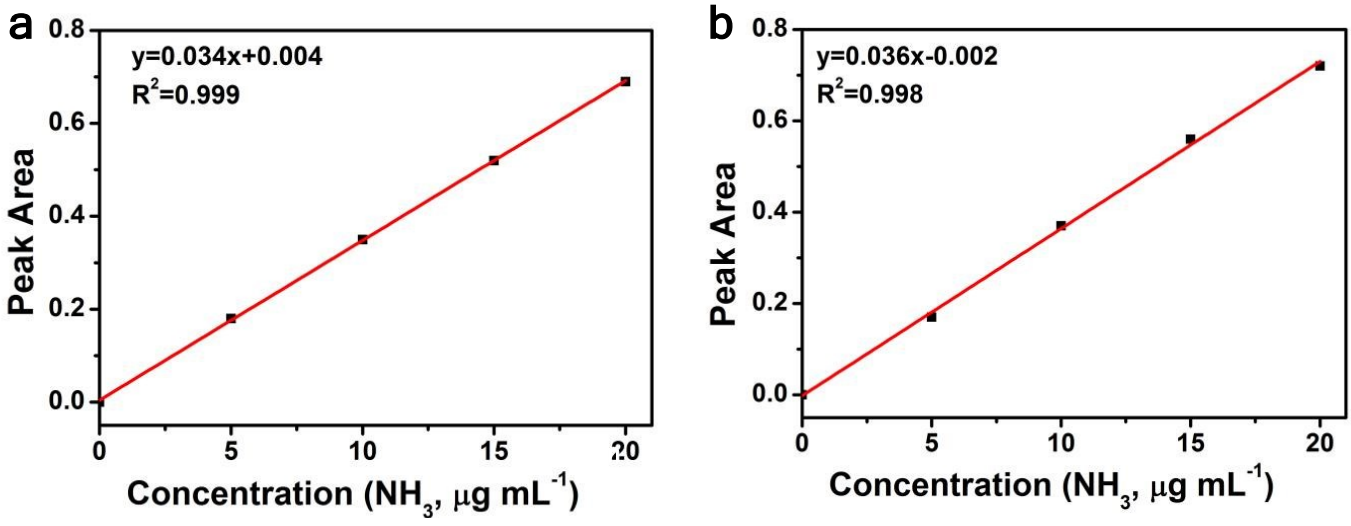

Figure S10. (a) Calibration curves for determination of $^{14}NH_4^+$. (b) Calibration curves for determination of $^{15}NH_4^+$.

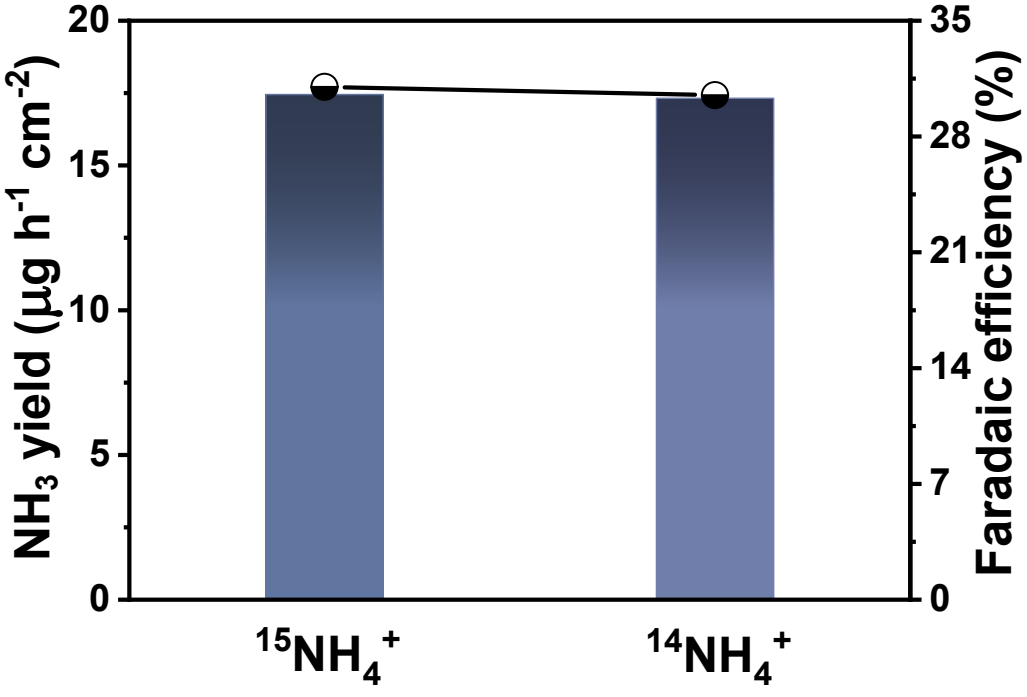

Figure S11. Comparison chart of $^{15}NH_4^+$ and $^{14}NH_4^+$ for NH_3 yield after 2 h electrolysis at -0.2 V.

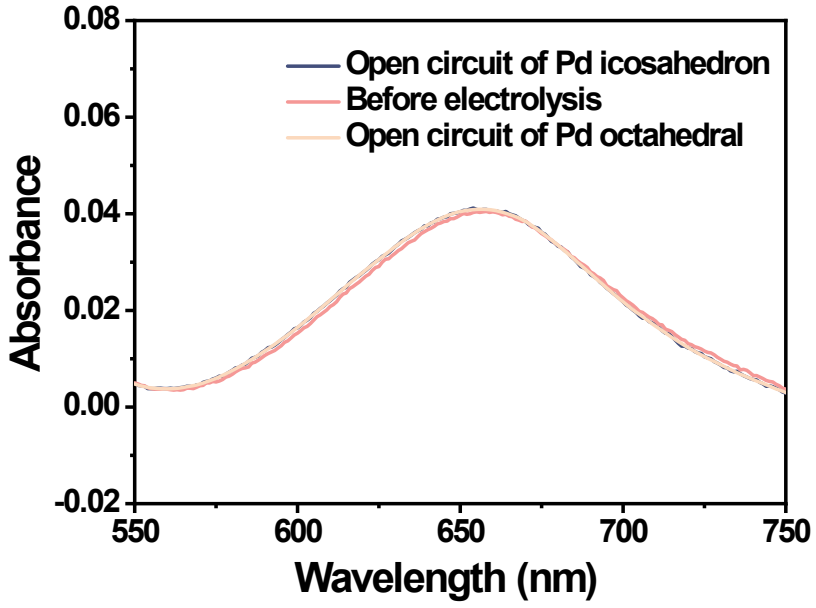

Figure S12. UV-Vis absorption spectra of Pd icosahedron and Pd octahedron in open circuit electrical test at -0.2 V (vs. RHE).

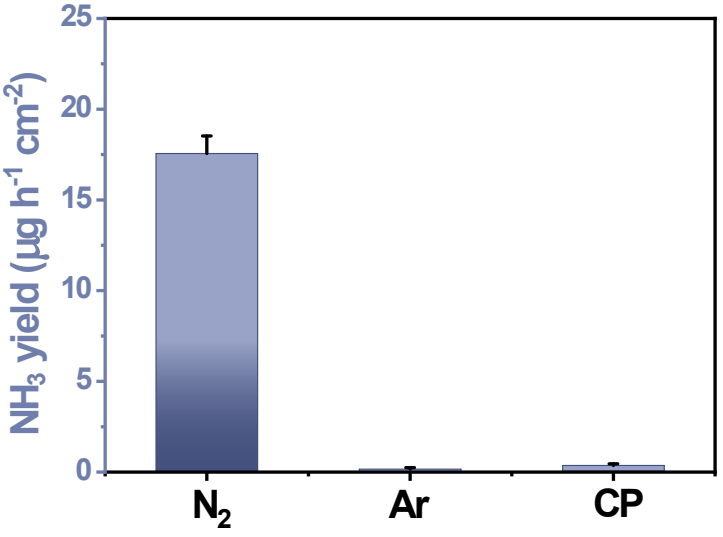

Figure S13. The yield of NH_4^+ after electrolysis for 2 h at -0.2 V vs. RHE.

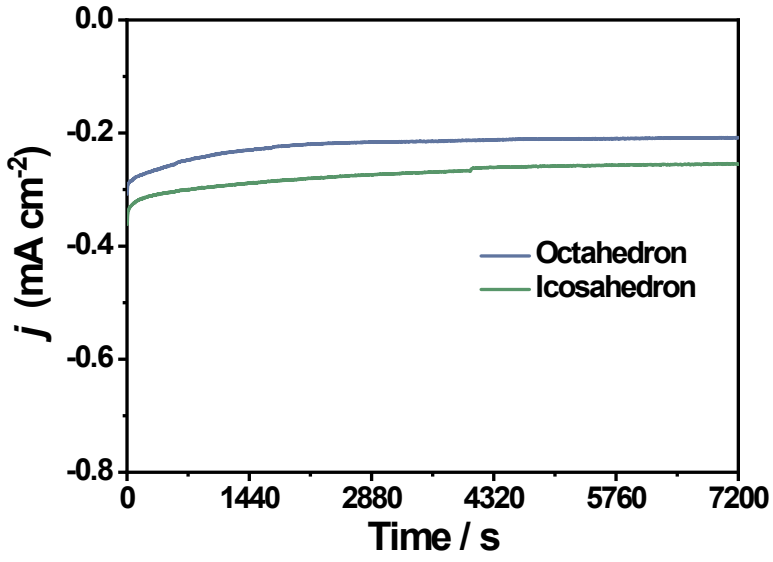

Figure S14. Chronoamperometry curves of Pd icosahedron and Pd octahedral at -0.2 V (vs. RHE).

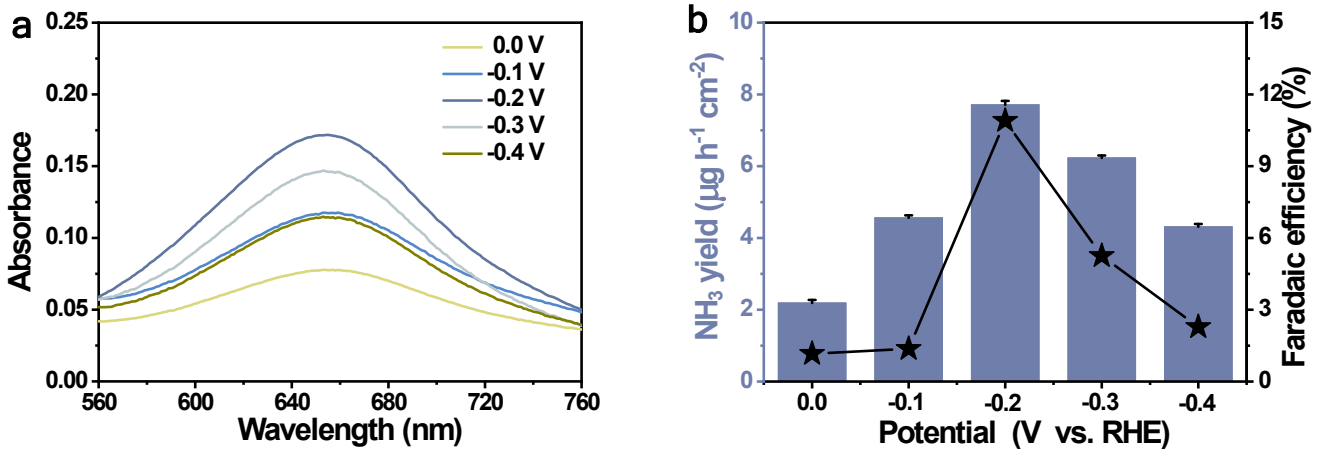

Figure S15. (a) UV-Vis absorption spectra of Pd octahedron at various potentials vs. RHE. (b) NH_3 yield rate and FE of Pd octahedron at various potentials vs. RHE.

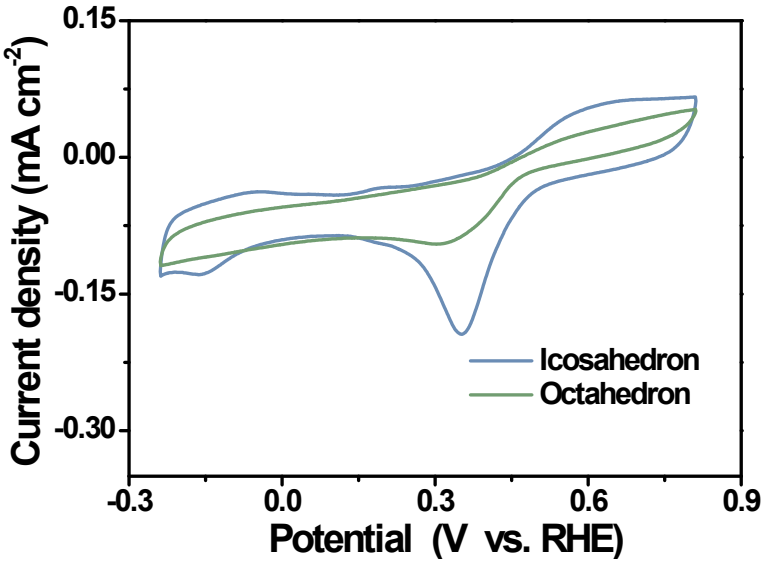

Figure S16. CV curves of Pd octahedrons and Pd icosahedron at a scan rate of 20 mV s^{-1} in 1 M KOH.

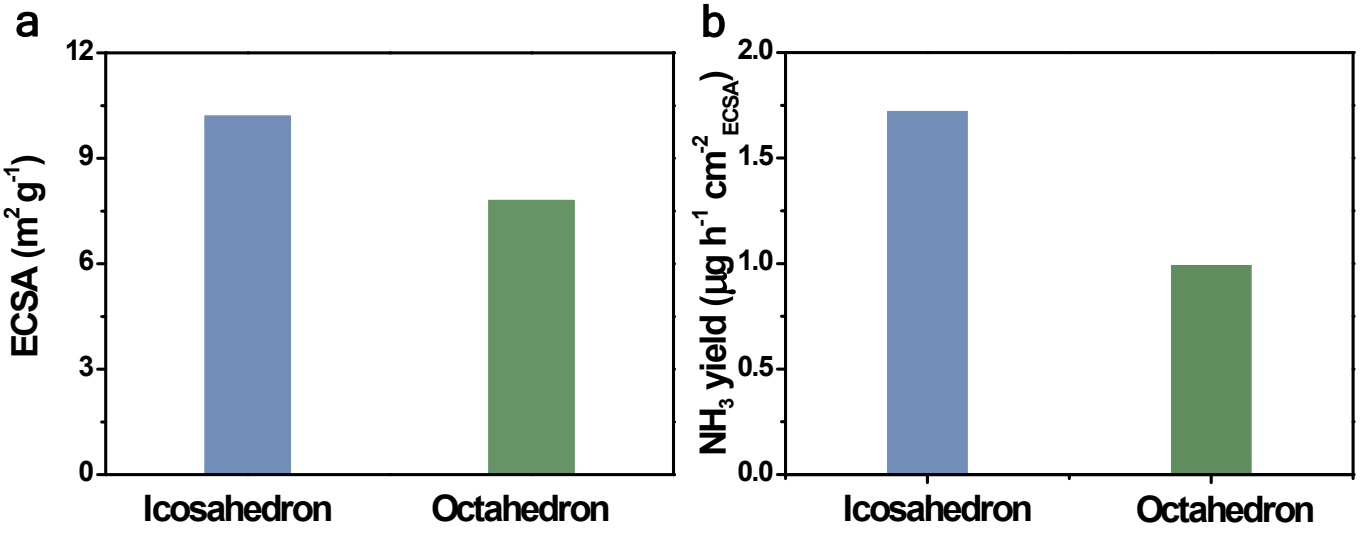

Figure S17. (a) Bar graph of ECSAs of different electrocatalysts. (b) The NH_3 area yields of different electrocatalysts by using their ESCAs.

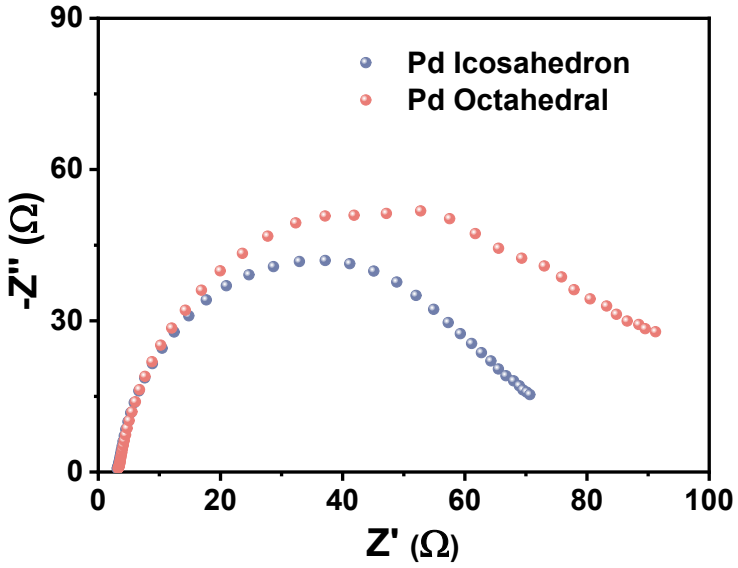

Figure S18. Electrochemical impedance spectroscopy (EIS) of Pd icosahedron and Pd octahedron.

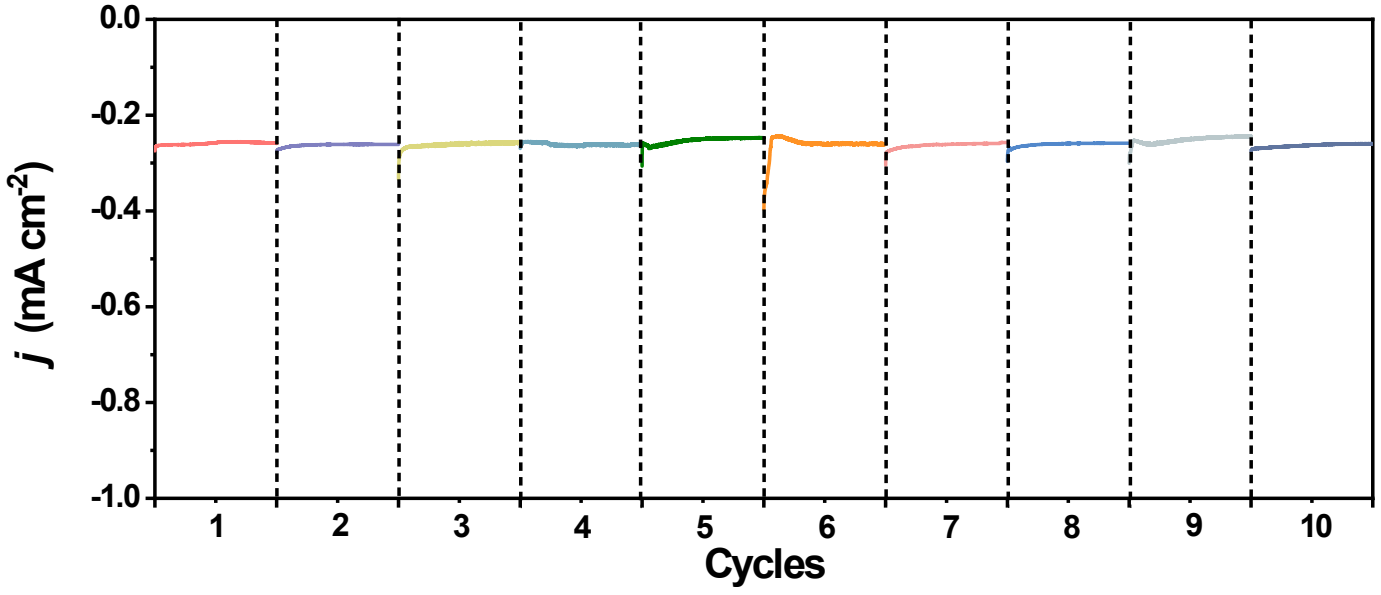

Figure S19. Time-dependent current density curves of Pd icosahedron with 2 h for each cycle in N_2-saturated 0.1 M Li_2SO_4.

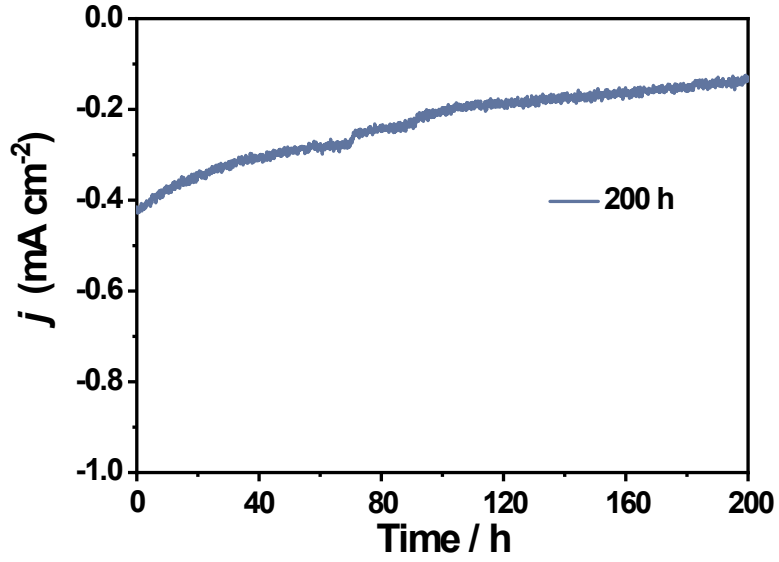

Figure S20. Time-dependent current density curve of Pd octahedron over for 200 h -0.2 V vs. RHE.

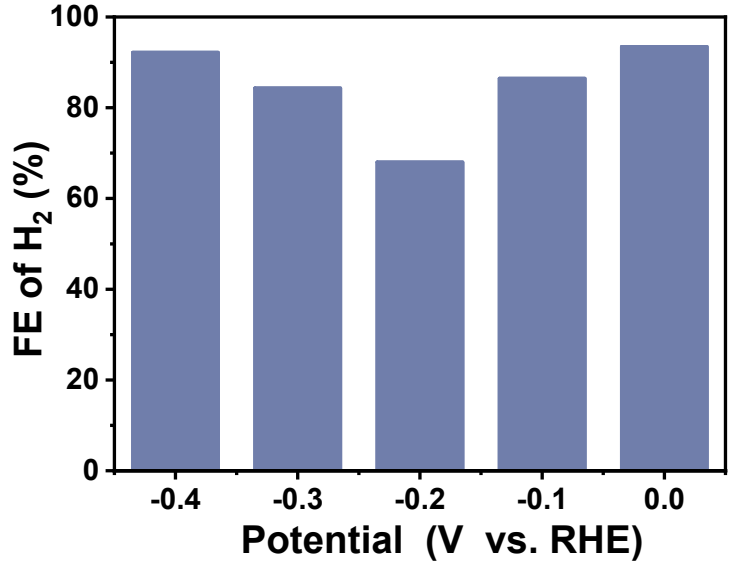

Figure S21. The FE of H_2 for Pd icosahedron at given potentials in 0.1 M Li_2SO_4.

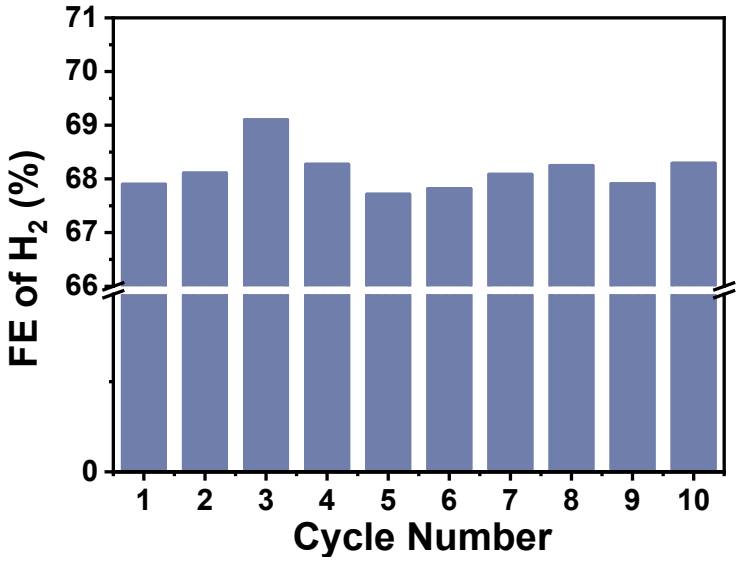

Figure S22. The FE of H_2 for Pd icosahedron at -0.2 V vs. RHE after cycling test.

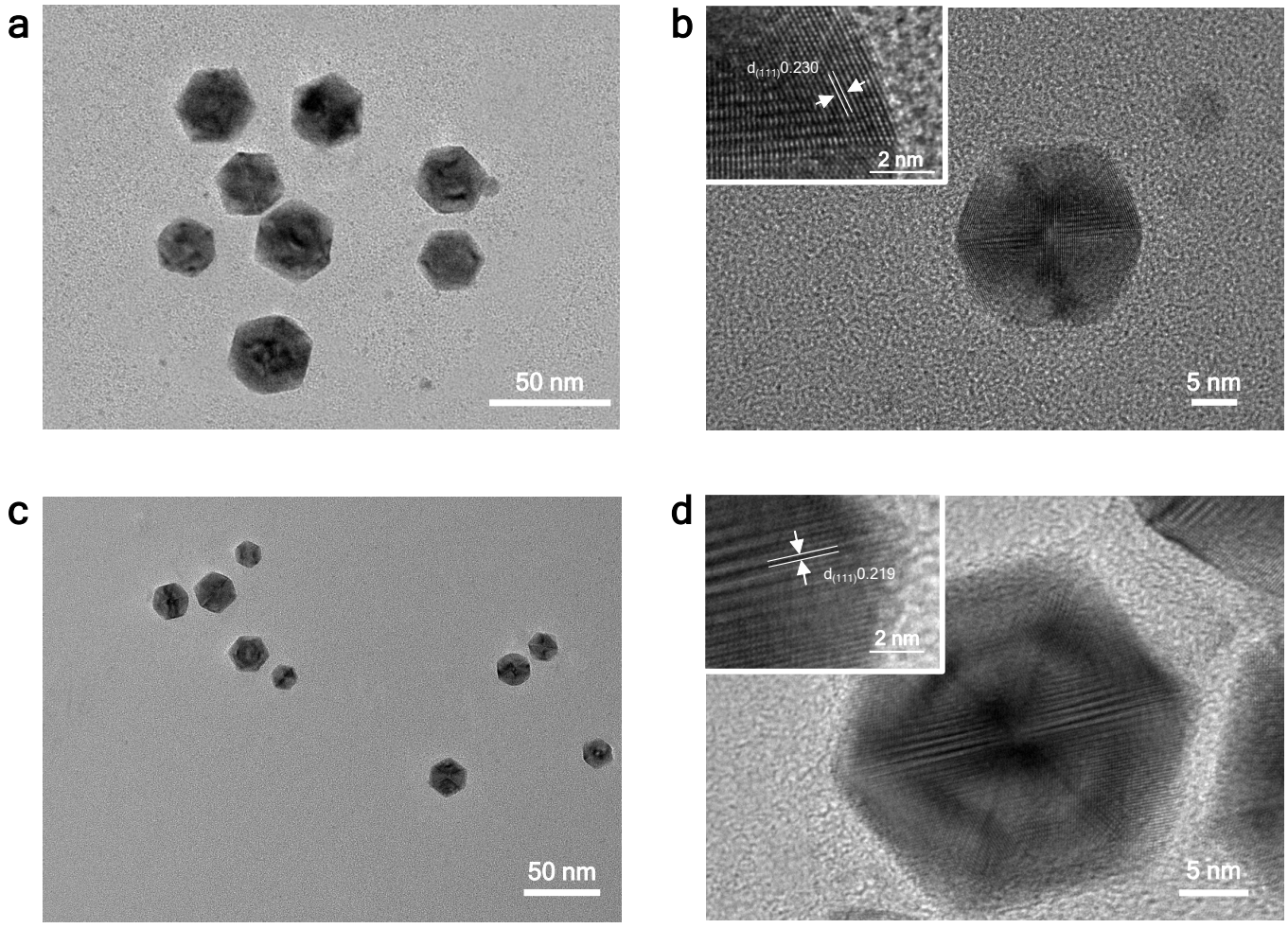

Figure S23. (a) The TEM image and (b) HRTEM image of Pd icosahedron catalyst after 200 h electrolysis; (c) The TEM image and (d) HRTEM image of Pd icosahedron catalyst after cycling test.

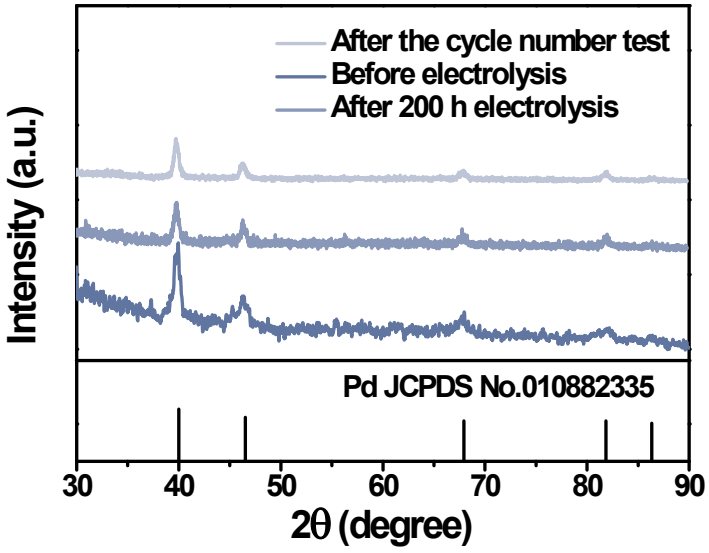

Figure S24. The XRD pattern of Pd icosahedron catalyst after NRR.

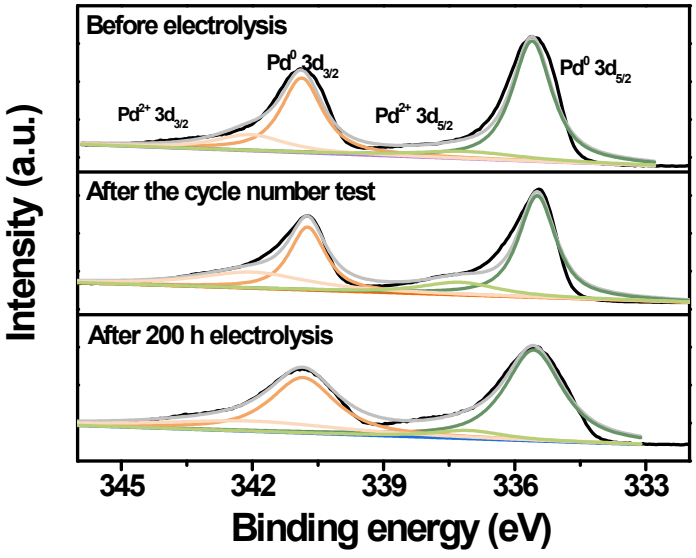

Figure S25. Pd 3d XPS spectra of Pd icosahedron before and after NRR.

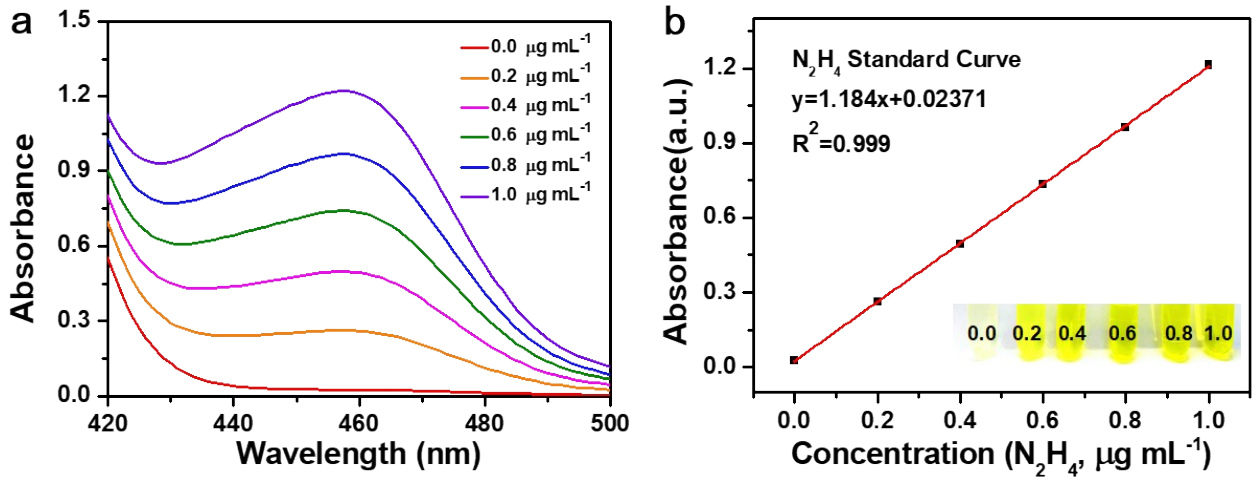

Figure S26. (a) The UV-Vis absorption spectra of indophenol assays with N_2H_4 after incubated for 10 min at room temperature. (b) Corresponding calibration curves for the colorimetric N_2H_4 assay in 0.1 M Li_2SO_4.

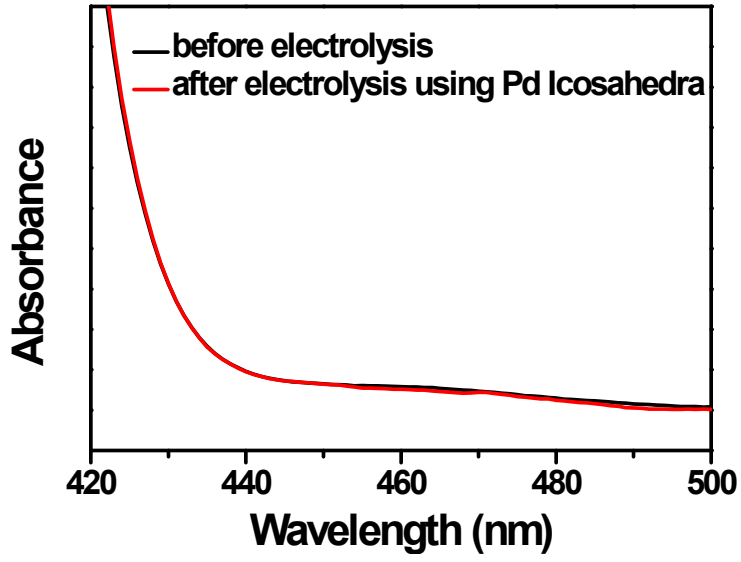

Figure S27. UV-Vis spectra of the electrolyte before and after electrolysis at -0.2 V vs. RHE.

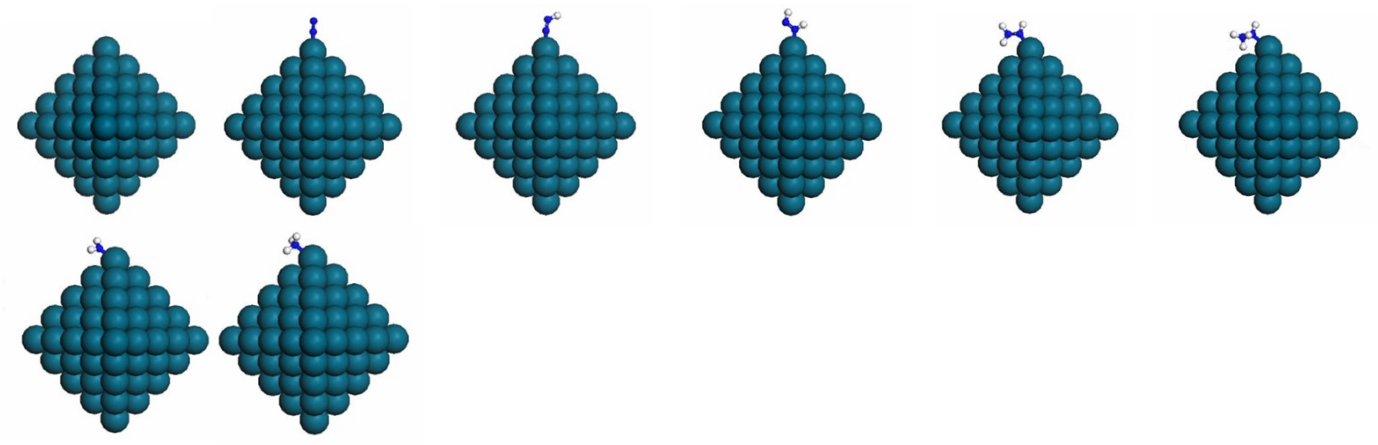

Figure S28. The reaction path carried out around the geometry of the Pd octahedrons intermediate.

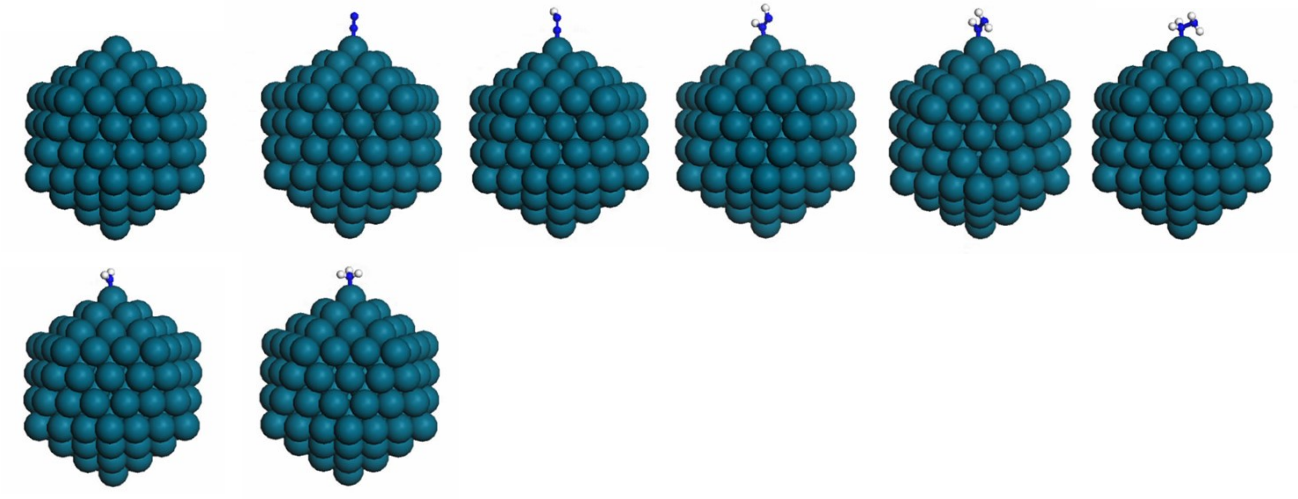

Figure S29. The reaction path carried out around the geometry of the Pd icosahedron intermediate.

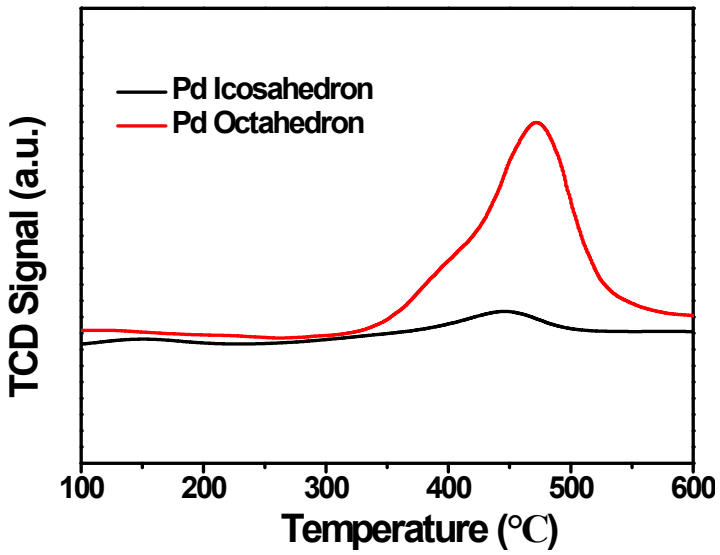

Figure S30. NH_3-TPD profiles of Pd icosahedron and Pd octachedron.

Table S1. The comparable results of our work and other recently reported NRR catalysts at the following potentials.

Catalyst	Conditions	Yield rate ($\mu g\ h^{-1}\ cm^{-2}$)	Faradaic efficiency (%)	Ref.
Pd icosahedral	0.1M Li_2SO_4 -0.2 V	17.56 (43.9 $\mu g\ h^{-1}\ mg_{cat.}^{-1}$)	31.98	This work
Pd octahedral	0.1M Li_2SO_4 -0.2 V	7.71 (19.3 $\mu g\ h^{-1}\ mg_{cat.}^{-1}$)	10.9	This work
RO-Cu_3P/CFC	0.1M Na_2SO_4 -0.2 V	10.6	14.3	[3]
Y_1/NC	0.1M HCl -0.2 V	16.9	3.7	[4]
Ni-Nx-C-700-3h	0.1M KOH -0.2 V	52	22	[5]
Mo SAs-Mo_2C	0.5M H_2SO_4 -0.2 V	11.6	7.3	[6]
Au NS (321)	0.1M KOH -0.2 V	2.6	10.2	[7]
Pt_3Fe NWs/C	0.1M KOH -0.2 V	0.2 $\mu g\ h^{-1}\ cm_{ECSA}^{-2}$	0.3	[8]
Ti_3C_2OH	0.1M KOH -0.2 V	1.71	7.01	[9]
Rh SA/GDY	0.1M K_2SO_4 -0.2 V	74.15 $\mu g\ h^{-1}\ mg^{-1}$	20.36	[10]
Au/o-CFP	0.1M Na_2SO_4 -0.2 V	26.3 $\mu g\ h^{-1}\ mg^{-1}$	27.2	[11]
Au_4Pd_2/G	0.1M HCl -0.2 V	27.1 $\mu g\ h^{-1}\ mg^{-1}$	12.3	[12]
Au-Fe_3O_4	0.1M KOH -0.2 V	21.42 $\mu g\ h^{-1}\ mg^{-1}$	10.54	[13]
PtMo-6	0.1M KOH -0.2 V	18.9 $\mu g\ h^{-1}\ mg^{-1}$	1.16	[14]

Table S2. The comparable results of our work and other recently reported NRR catalysts after long-term chronoamperometry testing.

Catalyst	Yield rate after short time electrolysis	Long electrolysis time	Yield rate after long time electrolysis	Ref.
Pd icosahedral	17.56 μg h^{-1} cm^{-2} (43.9 μg h^{-1} $mg_{cat.}^{-1}$)	200 h	15.22 μg h^{-1} cm^{-2}	This work
Pd octahedron	7.71 μg h^{-1} cm^{-2} (19.3 μg h^{-1} $mg_{cat.}^{-1}$)	200 h	1.56 μg h^{-1} cm^{-2}	This work
Fe-SAs/LCC/CC	32.1 μg h^{-1} mg^{-1}	120 h	25.23 μg h^{-1} mg^{-1}	[15]
RO-Cu_3P/CFC	40.6 μg h^{-1} mg^{-1}	24 h	40.1 μg h^{-1} mg^{-1}	[11]
Ti_3C_2OH	1.71 μg h^{-1} cm^{-2}	18 h	1.20 μg h^{-1} cm^{-2}	[9]
Rh_2P@NPC	37.6 μg h^{-1} mg^{-1}	48 h	34.3 μg h^{-1} mg^{-1}	[16]
c-TiO_2 NAs	4.19×10^{-10} mol s^{-1} cm^{-2}	24 h	3.68×10^{-10} mol s^{-1} cm^{-2}	[17]
S-NV-C_3N_4	32.7 μg h^{-1} mg^{-1}	20 h	29.5 μg h^{-1} mg^{-1}	[18]
Fe-CeO_2	26.2 μg h^{-1} mg^{-1}	15 h	23.9 μg h^{-1} mg^{-1}	[19]
Sb_2Te_3/CP	13.8 μg h^{-1} cm^{-2}	50 h	12.6 μg h^{-1} cm^{-2}	[20]

References

1 L. Zhang, L. Ding, G. Chen, X. Yang, H. Wang, *Angew. Chem. Int. Ed.* 2018, **58**, 2612-2642.

2 X. Zhu, T. Wu, L. Ji, C. Li, T. Wang, S. Wen, S. Gao, X. Shi, Y. Luo, Q. Peng, X. Sun, *J. Mater. Chem. A* 2019, **7**, 16117.

3 M. Jin, X. Zhang, M. Han, H. Wang, G. Wang, H. Zhang, *J. Mater. Chem. A* 2020, **8**, 5936-5942.

4 J. Liu, X. Kong, L. Zheng, X. Guo, X. Liu, J. Shui, *ACS Nano* 2020, **14**, 1093-1101.

5 S. Mukherjee, X. Yang, W. Shan, W. Samarakoon, S. Karakalos, D. A. Cullen, K. More, M. Wang, Z. Feng, G. Wang, G. Wu, *Small Methods* 2020, **4**, 1900821.

6 Y. Ma, T. Yang, H. Zou, W. Zang, Z. Kou, L. Mao, Y. Feng, L. Shen, S. J. Pennycook, L. Duan, X. Li, J. Wang, *Adv. Mater.* 2020, **32**, 2002177.

7 W. Zhang, Y. Shen, F. Pang, D. Quek, W. Niu, W. Wang, P. Chen, *ACS Appl. Mater. Interfaces* 2020, **12**, 41613-41619.

8 W. Tong, B. Huang, P. Wang, Q. Shao, X. Huang, *Natl. Sci. Rev.* 2020, **4**, 1336-1341.

9 J. Xia, S. Yang, B. Wang, P. Wu, I. Popovs, H. Li, S. Irle, S. Dai, H. Zhu, *Nano Energy* 2020, **72**, 104681.

10 H. Zou, W. Rong, S. Weia, Y. Jic, L. Duan, *Proc. Natl. Acad. Sci. U.S.A.* 2020, **117**, 29462-29468.

11 J. Zhang, B. Zhao, W. Liang, G. Zhou, Z. Liang, Y. Wang, J. Qu, Y. Sun, L. Jiang, *Adv. Sci.* 2020, **7**, 2002630.

12 C. Yao, N. Guo, S. Xi, C. Q. Xu, W. Liu, X. Zhao, J. Li, H. Fang, J. Su, Z. Chen, H. Yan, Z. Qiu, P. Lyu, C. Chen, H. Xu, X. Peng, X. Li, B. Liu, C. Su, S. J. Pennycook, C. J. Sun, J. Li, C. Zhang, Y. Du, J. Lu, *Nat. Commun* 2020, **11**, 4389.

13 J. Zhang, Y. Ji, P. Wang, Q. Shao, Y. Li, X. Huang, *Adv. Funct. Mater.* 2019, **30**, 1906579.

14 Xu Guo, X. Li, Y. Li, J. Yang, X. Wan, L. Chen, J. Liu, X. Liu, R. Yu, L. Zheng, J. Shui, *Nano Energy* 2020, **78**, 105211.

15 H. Zhao, S. Zhang, M. Jin, T. Shi, M. Han, Q. Sun, Y. Lin, Z. Ding, L. R. Zheng, G. Wang, Y. Zhang, H. Zhang, *Angew. Chem. Int. Ed. Engl.* 2020.

16 J. Su, H. Zhao, W. Fu, W. Tian, X. Yang, H. Zhang, F. ling, Y. Wang, *Appl. Catal. B: Environ.* 2020, 118589.

17 Y. Liu, M. Zhang, Y. Wang, Y. Zhang, J. Song, Y. Si, J. Yan, C. Ma, J. Yu, B. Ding, *Angew. Chem. Int. Ed. Engl.* 2020, **59**, 23252-23260.

18 K. Chu, Q. Li, Y. Liu, J. Wang, Y. Cheng, *Appl. Catal. B: Environ.* 2020, **267**, 118693.

19 K. Chu, Y. Cheng, Q. Li, Y. Liu, Y. Tian, *J. Mater. Chem. A* 2020, **8**, 5865-5873.

20 Y. Han, W. Cai, X. Wu, W. Qi, B. Li, H. Li, D. Zhang, Y. Pan, Z. Wang, J. Lai, L. Wang, *Cell Reports Phys. Sci* 2020, **1**, 100232.